A Mechanism for Extrusion Instabilities in Polymer Melts

M. FYRILLAS

Faculty of Applied Physics, Rheology Group
University of Twente, P.O. Box 217
7500 AE Enschede, The Netherlands

G. GEORGIOU*

Department of Mathematics and Statistics
University of Cyprus, P.O. Box 20537
1678 Nicosia, Cyprus

D. VLASSOPOULOS

Foundation for Research and Technology-Hellas (FO. R. T. H.)
Institute of Electronic Structure and Laser, P.O. Box 1527
71110 Heraklion, Crete, Greece

S. HATZIKIRIAKOS

Department of Chemical Engineering
The University of British Columbia, 2216 Main Mall
Vancouver, BC, V6T-1Z4, Canada

A mechanism for explaining some of the instabilities observed during the extrusion of polymer melts is further explored. This is based on the combination of non-monotonic slip and elasticity, which permits the existence of periodic solutions in viscometric flows. The time-dependent, incompressible, one-dimensional plane Poiseuille flow of an Oldroyd-B fluid with slip along the wall is studied using a non-monotonic slip equation relating the shear stress to the velocity at the wall. The stability of the steady-state solutions to one-dimensional perturbations at fixed volumetric flow rateis analyzed by means of a linear stability analysis and finite element calculations. Self-sustained periodic oscillations of the pressure gradient are obtained when an unstable steady-state is perturbed, in direct analogy with experimental observations.

INTRODUCTION

It is well known that during the capillary extrusion of polymers underfixed piston speed, when the wall shearstress exceeds a critical value and the apparent shear rate falls within a certain range, unstable flow commences (1–4). In a certain piston speed range, the pressure drop oscillates between two extreme values although the flow rate is kept constant. This instability is believed to be due to a transition from a weak slip to a strong slip in combination with the small but finite compressibility of polymers (1–5). *Figure 1* depicts a typical flow curve (i.e., the plot of the wall shear stress σ_w versus the apparent shear rate $\dot{\gamma}_A$ at the wall) for a linear polyethylene. Such a curve is determined routinely by using a capillary rheometer

*Corresponding author.

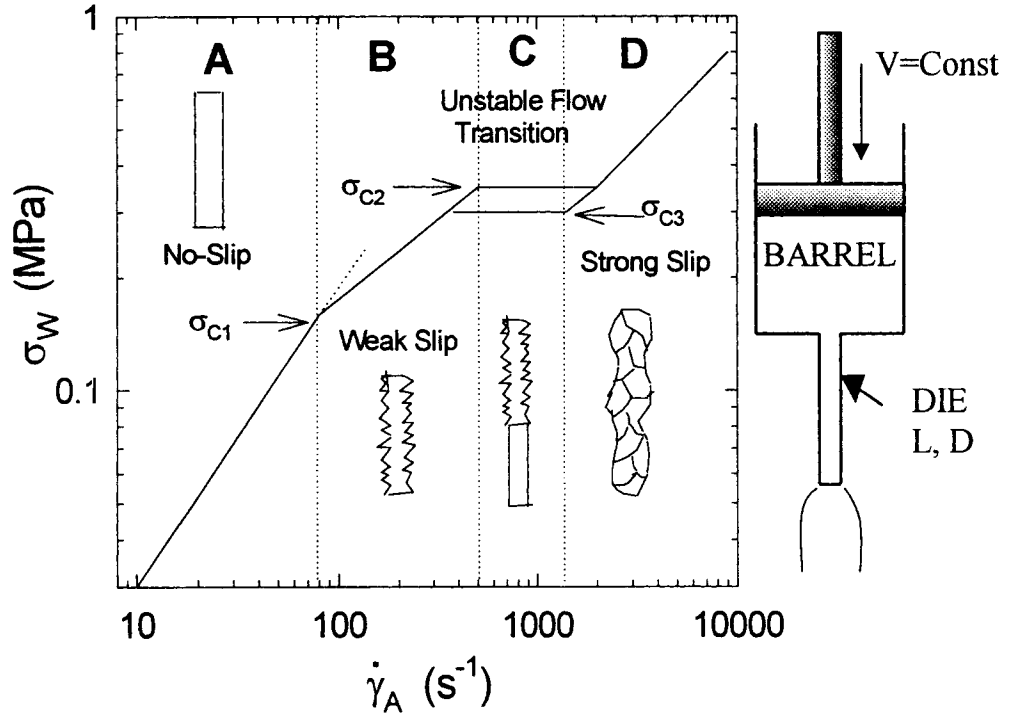

Fig. 1. A typical flow curve of a linear polyethylene as determined by a capillary rheometer.

under constant piston speed operation. The piston speed is fixed and the pressure drop required to attain steady-state operation is recorded.

Apart from a Newtonian flow region (not shown in *Fig. 1*), which is identified at very low apparent shear rates, four distinct flow region scan, in general, be observed. At small shear rates (flow region A), the polymer emerging from the capillary die is glossy and smooth upon cooling, and the classical no-slip boundary condition of fluid mechanics is a valid assumption. At higher shear rates and more specifically for wall shear stresses greater than a critical value σ_{C1} (region B), there is a sharp change in the slope of the flow curve that is mainly due to a small departure from the no-slip boundary condition (weak slip). The extrudate starts loosing gradually its glossiness and small amplitude periodic distortions appear on its surface (*surface melt fracture* or *sharkskin*). The mechanism of slip in this flow region is apparently due to flow-induced chain detachment/desorption from the interface (7). The number of desorbed chains increases with an increase of shear stress/shear rate, and as a result the slip velocity increases accordingly. For wall shear stresses greater than a second critical value, σ_{C2}, and within a certain range of apparent shear rates, the flow becomes unstable (region C in *Fig. 1*, known as *oscillating melt fracture* flow region). Sustained pressure oscillations, due to the combined effects of the finite compressibility of the polymer and the transition from a weak slip (region B) to a strong slip (region D), are observed. This slip transition reflects the sudden disentanglement of the polymer chains in the bulk from a monolayer of polymer chains adsorbed at the interface (8). When the shear stress relaxes and assumes a third critical value, another transition takes place, this time from a strong slip (region D) to a weak slip (B) due to there-establishment of entanglements at the interface. As a result, a hysteresis loop is obtained. In this flow regime, alternate distorted and smooth zones appear on the extrudate surface. Finally, at even higher wall shear stress values the flow becomes again stable (region D), although the extrudate assumes a chaotic appearance (*gross melt fracture*). In this flow regime, the flow can be approximated by a flat velocity profile, i.e., the flow is almost plug.

From the above, it is clear that unlike Newtonian fluids, polymers slip over solid surfaces when the wall shear stress exceeds a critical value (4–6). For the case of a passive interface (no interaction between the polymer and solid surface), de Gennes (9) first proposed an interfacial rheological law in terms of an extrapolation length. If a linear expression between the slip velocity and wall shear stress is assumed, it may easily be deduced that the extrapolation length should scale with the viscosity of the polymer at constant shear stress values (9, 10). This theory has recently been extended by Brochard-Wyart and de Gennes (11) to distinguish a passive interface (no polymer adsorption) from an adsorbing one. It has been predicted that there exists a critical wall shear stress value at which a transition from a weak to a strong slip takes place. This result is in agreement with experimental observations (4, 8, 10, 12).

Therefore, the flow of polymer melts is governed by two slip mechanisms. The first slip mode, which accounts for relatively small deviations from the no-slip boundary condition, is observed macroscopically at relatively small values of the wall shear stress and is attributed to the direct detachment/desorption of a few chains from the wall (7, 13, 14). The second mode, i.e. the transition from a weak to a strong slip, is attributed to sudden disentanglement of the polymer chains in the bulk from those in a monolayer of polymer chains adsorbed at the wall (8, 10). Both mechanisms are still being studied actively by many groups.

It is emphasized that the various flow regimes of *Fig. 1*, and in particular the stick-slip flow, can be observed under constant piston speed operation, i.e., at constant volumetric flow rate. The origin of the instabilities has been a controversial and not yet fully resolved issue. Pearson (15) first pointed out that the combination of nonmonotonic slip with compressibility can lead to self-sustained oscillations of the pressure drop in Poiseuille flow. Georgiou and Crochet (16, 17) demonstrated numerically this instability mechanism solving the compressible, two-dimensional Newtonian Poiseuille and extrudate-swell flows. Kumar and Graham used a one-dimensional relaxation model in order to describe the oscillations of the pressure and the volumetric flow rate in the stick-slip regime [(18) and references therein]. This model includes the reservoir region and takes into account the compressibility of the fluid. The authors modified the slip equation used by Georgiou and Crochet (16), in order to include the pressure dependence of the slip velocity, and considered both generalized Newtonian and viscoelastic fluids (18).

Recently, Shore *et al.* (19, 20) presented a hydrodynamic model describing the Poiseuille flow of a viscoelastic Maxwell fluid, under the assumption that the polymer near the surface undergoes a first-order transition in conformation as the wall shear stress increases. This conformational change produces stick-slip behavior and leads to an effectively multivalued flow curve. Shore *et al.* (19, 20) considered the linearized, incompressible, two-dimensional Navier-Stokes equations assuming periodic conditions in the direction of the flow and demonstrated the existence of self-sustained oscillations and their relationship to sharkskin texturing, by means of linear stability analysis and numerical simulations. Black and Graham (21) have also demonstrated that the combination of slip and elasticity leads to unstable solutions. They employed a simple phenomenological evolution equation for the slip process and carried out a linear stability analysis for the creeping, plane, incompressible Couette flow of the upper convected Maxwell fluid.

In this paper, we explore further an instability mechanism which is based on the combination of nonlinear slip and elasticity (22–24). We consider the time-dependent, incompressible, one-dimensional plane Poiseuille flow of an Oldroyd-B fluid. The Oldroyd-B model exhibits a monotonic steady shear response, and involves the upper convected Maxwell model as a trivial case. We use a slip law which captures several of the experimentally observed features and assumes that slip depends only on the shear stress through a multivalued relation. Note that the slip model employed by Black and Graham (21) is single valued and involves normal stress dependence which is necessary for instability. In contrast to the work of Shore *et al.* (19, 20), the existence of periodic solutions in the linearly unstable regime is demonstrated in the case of the one-dimensional flow, without the use of periodic conditions in the direction of the flow.

THE PROPOSED MODEL

Governing Equations and Boundary Conditions

Let lengths be scaled by the half-width H of the slit, the velocity vector $\mathbf{v}$ by a characteristic velocity V, the pressure and the stress components by $\eta V/H$, where η is the shear viscosity, and the time t by H/V. The dimensionless x-momentum equation is

$$Re\frac{\partial v_x}{\partial t} = -\nabla P + \frac{\partial T_1^{xy}}{\partial y} + \eta_2\frac{\partial^2 v_x}{\partial y^2}, \tag{1}$$

where ∇P denotes the dimensionless pressure gradient, Re is the Reynolds number given by

$$Re \equiv \frac{\rho VH}{\eta}, \tag{2}$$

and ρ is the density. $\mathbf{T_1}$ is the viscoelastic part of the stress tensor $\mathbf{T}$, so that

$$\mathbf{T} = \mathbf{T_1} + \eta_2[(\nabla\mathbf{v}) + (\nabla\mathbf{v})^T], \tag{3}$$

where η_2 is a dimensionless viscosity parameter (scaled by the shear viscosity η), $\nabla\mathbf{v}$ is the velocity-gradient tensor, and the superscript T denotes the transpose. For the xy-component T_1^{xy} of $\mathbf{T_1}$, one obtains

$$T_1^{xy} + We\frac{\partial T_1^{xy}}{\partial t} = \eta_1\frac{\partial v_x}{\partial y}, \tag{4}$$

where We is the Weissenberg number, defined by

$$We \equiv \frac{\lambda V}{H}, \tag{5}$$

λ is the relaxation time, and $\eta_1 = 1 - \eta_2$ is another dimensionless viscosity parameter. Along the symmetry plane ($y = 0$), the velocity gradient is zero. Along the wall, we assume that slip occurs following a law of the general form

$$\sigma_w = -F(v_w) \quad \text{at} \quad y = 1, \tag{6}$$

where v_w is the slip velocity.

Steady-State Solution

The solution of the steady-state problem (*Eqs 1–2*) is:

$$v_x = v_w - \frac{1}{2}\nabla P(1 - y^2), \tag{7}$$

and

$$T^{xy} = T_1^{xy} + \eta_2 \frac{\partial v_x}{\partial y} = \nabla P\, y, \tag{8}$$

where the slip velocity v_w satisfies the condition

$$\sigma_w = \nabla P = -F(v_w). \tag{9}$$

The volumetric flow rate Q is given by

$$Q = v_w - \frac{1}{3}\nabla P = v_w + \frac{1}{3}F(v_w). \tag{10}$$

We now consider the arbitrary nonmonotonic slip equation (16, 17)

$$\sigma_w = -F(v_w) = -A_1\left(1 + \frac{A_2}{1 + A_3 v_w^2}\right)v_w. \tag{11}$$

In *Fig. 2*, we show the nonmonotonic flow curve corresponding to $A_1 = 1$, $A_2 = 15$ and $A_3 = 100$. For fixed volumetric flow rate, integrating the x-momentum *Eq 1* over the cross section of the slit yields

$$-\nabla P = F(v_w) \quad \forall\, t\,. \tag{12}$$

Therefore, the time-dependent pressure gradient follows the steady-state curve of ∇P vs v_w, exactly as has been observed experimentally (13).

Time-Dependent Solution for Re = 0

In the case of creeping flow ($Re = 0$), the time-dependent solution is given by

$$v_x = v_w + \frac{3}{2}(Q - v_w)(1 - y^2), \tag{13}$$

and

$$T_1^{xy} = -F(v_w)y + 3\,\eta_2(Q - v_w)y, \tag{14}$$

i.e. the shear stress is linear and the velocity v_x is parabolic at all times. If the steady-state slip velocity $\bar{v}_w$ is perturbed to v_w^0 and the derivative $F'(v_w)$ is locally constant, one obtains from *Eq 1*:

$$v_w = \bar{v}_w + (v_w^0 - \bar{v}_w)\exp\left\{-\frac{3 + F'(\bar{v}_w)}{We\,[3\eta_2 + F'(\bar{v}_w)]}t\right\}. \tag{15}$$

When $-3\eta_2 < F'(v_w) < 0$, the flow is stable for all values of v_w. Note also that the points where $F'(\bar{v}_w) = -3\,\eta_2$ are limit points. A steady solution on the right stable branch cannot be reached if calculations start from a point to the left of a limit point, and vice versa. In the case of the Maxwell fluid, $\eta_2 = 0$ and the limit points are the extrema of $F(v_w)$.

Linear Stability Analysis

The stability of the steady-state solutions to infinitesimal one-dimensional antisymmetric disturbances at fixed volumetric flow rate was first studied by means of a linear stability analysis. The neutral stability curves for various values of η_2 are plotted in *Fig. 3*. The procedure for constructing the neutral stability curves is analogous to that for the case of simple shear flow (23).

It is clear that the stability of a basic solution depends on three parameters: η_2, $F'(\bar{v}_w)$ and the elasticity number, ε, defined by

$$\varepsilon \equiv \frac{We}{Re}. \tag{16}$$

Unstable solutions exist only when $F'(\bar{v}_w)$ is negative and above the corresponding marginal stability curve. The flow is stable for a Newtonian fluid ($\eta_2 = 1$) and destabilizes as η_2 is decreased. The size of the instability regime is increased with the elasticity number ε. As already mentioned, in the limit of zero Reynolds

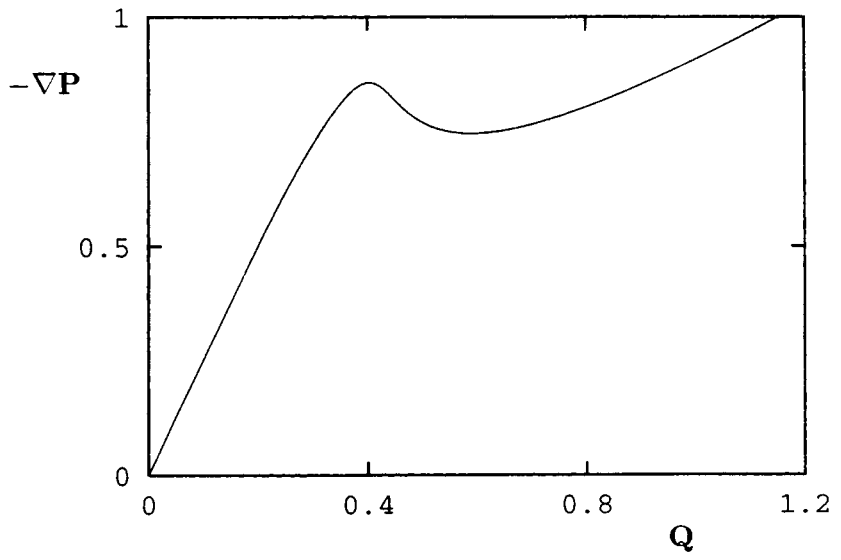

Fig. 2. Flow curve for $A_1 = 1$, $A_2 = 15$ and $A_3 = 100$.

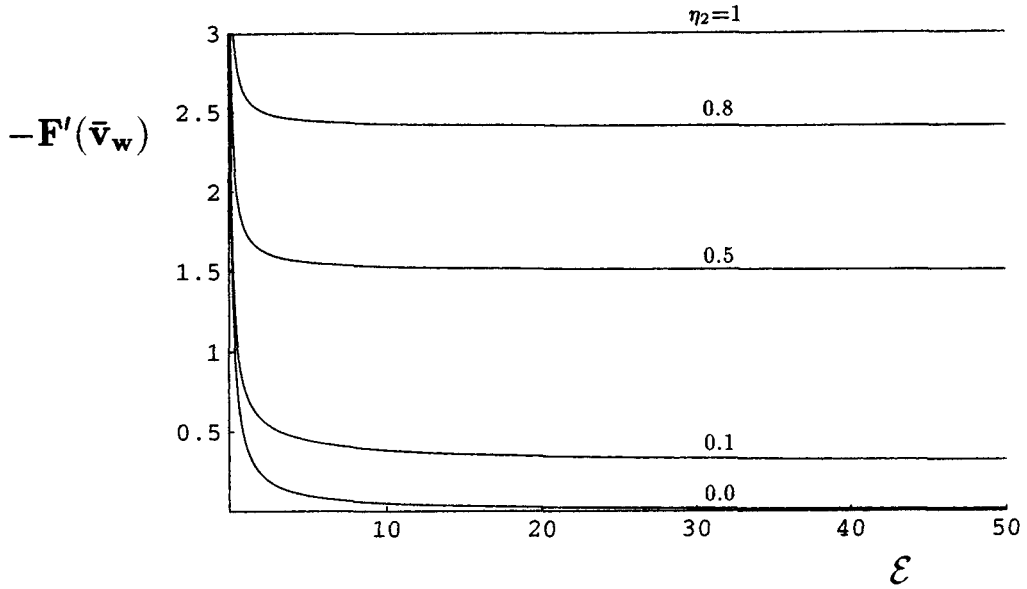

Fig. 3. Stability curves for the plane Poiseuille flow of an Oldroyd-B fluid with slip along the wall. The flow is unstable above the corresponding curve and stable below. The curves go to $3\eta_2$ as $\varepsilon \to \infty$.

number ($\varepsilon \to \infty$), the steady-state solutions are unstable when $F'(\bar{v}_w) < -3\eta_2$. Hence, the stability curves of *Fig. 3* approach asymptotically the value $3\eta_2$.

NUMERICAL RESULTS

To solve the system of *Eqs 1* and *4* numerically, we employ standard finite elements in space and the Euler backward difference scheme in time. We approximate both v_x and T_1^{xy} in terms of quadratic basis functions using a uniform mesh with 400 elements.

The time-dependent calculations are in excellent agreement with the predictions of the linear stability analysis, i.e., steady-state solutions above the marginal stability curves of *Fig. 3* are unstable. If such a solution is perturbed, periodic oscillations of the pressure gradient are obtained. Elasticity acts as the storage of elastic energy leading to self-sustained oscillations of the pressure drop and to transitions from weak to strong slip and vice versa.

In *Fig. 4*, we show results obtained with $A_1 = 1$, $A_2 = 15$ and $A_3 = 100$, $Re = 0.1$, $We = 1$ and $\eta_2 = 0.1$. We plot the evolution of the slip velocity and the pressure gradient when we start from the steady-state solution for $Q_0 = 0.449$ and set $Q = 0.45$ at $t = 0$; the latter value of the volumetric flow rate Q corresponds to the negative slope regime of the flow curve (*Fig. 2*). Similar results have been obtained with much lower Reynolds numbers. Notice that, in general, the same periodic solution is obtained when Q_0 is much further away from Q, say on one of the two positive-slope branches of the slip equation. In *Fig. 4a*, we observe that the slip velocity jumps from low (weak slip) to high values (strong slip); when the slip velocity is at a maximum the flow is almost plug. A good test for the accuracy of the time-dependent calculations is to plot the pressure gradient versus the slip velocity (*Fig. 4c*), in order to verify that, indeed, these two quantities move along the steady-state flow curve, as required by *Eq 12*. The local minima of the pressure gradient in *Fig. 4b* are caused by the fact that the oscillations extend to a small part of the left positive-slope part of the flow curve (*Fig. 4c*).

The effect of the elasticity on the amplitude and the period of the oscillations has also been studied. Both quantities decrease as *We* is decreased, and below a critical value the solution becomes stable, in good agreement with the linear stability analysis. Finally, our calculations show that the amplitude and the frequency of the oscillations increase when the Reynolds number is reduced. Since the definition of the Reynolds number involves a characteristic velocity coming from the arbitrary slip equation (*Eq 11*), a detailed study of the Reynolds number effect has not been pursued in the present work.

CONCLUSIONS

In summary, our numerical calculations show that, indeed, the combination of nonmonotonic slip at the wall with elasticity produces, above a threshold volumetric flow rate value, self-sustained oscillations of the pressure drop, in qualitative agreement with the existing experimental evidence (1–4). The proposed mechanism can thus provide a reasonable explanation for the main features of the stick-slip instability and opens the route for testing more realistic but less tractable computationally constitutive equations together with a realistic slip equation for analyzing the flows of entangled melts (25). The proposed mechanism might be proved useful in explaining similar instability phenomena encountered with other soft materials such as surfactants (26).

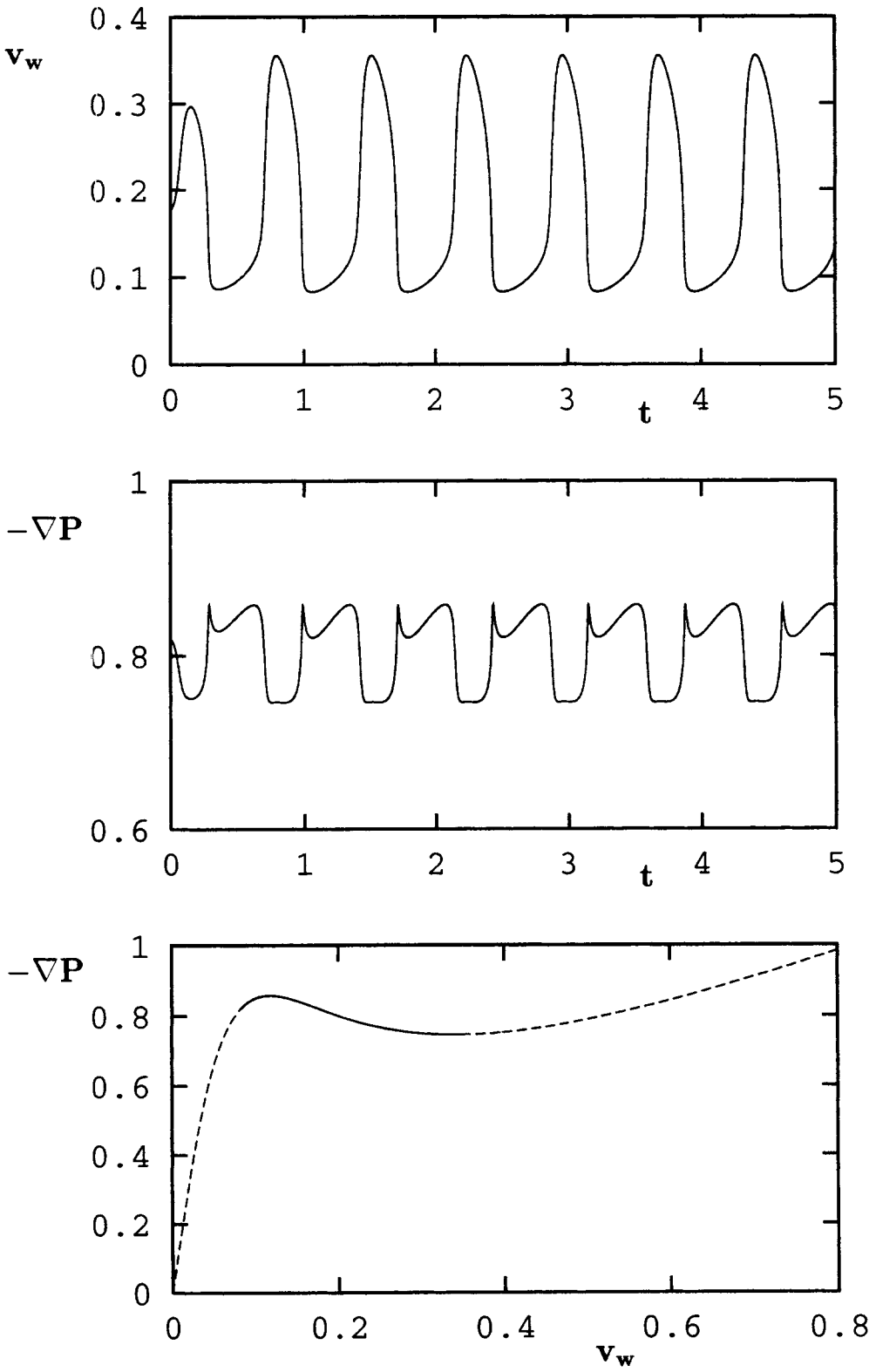

Fig. 4. Evolution of the solution when the unstable steady-state solution for $Q^0 = 0.449$ is perturbed by setting $Q = 0.45$ at $t = 0$; $Re = 0.1$, $We = 1$ and $\eta_2 = 0.1$. The dashed line in the last plot is the steady-state solution.

Any realistic simulation of extrusion instabilities should include the reservoir and extrudate regions. The former region is needed in order to account for reservoir volume effects, i.e., for compressibility effects (16, 18). The latter is, of course, necessary for studying the resulting oscillations of the extrudate surface which is the ultimate goal of the simulation (24).

ACKNOWLEDGMENTS

Part of this research was supported by the Operational Research Program of Crete, PEP 1994-98 (project N112115).

REFERENCES

1. E. B. Bagley, I. M. Cabott, and D. C. West, *J. Appl. Phys.*, **29**, 109 (1958).
2. W. R. Schowalter, *J. Non-Newtonian Fluid Mech.*, **29**, 25 (1978).
3. D. De Kee and K. F. Wissbrun, *Physics Today*, **51**, 24 (1998).
4. A. V. Ramamurthy, *J. Rheol.*, **30**, 337 (1986).
5. S. G. Hatzikiriakos and J. M. Dealy, *J. Rheol.*, **36**, 845 (1992).
6. J. R. Barone, N. Plucktaveesak, and S. Q. Wang, *J. Rheol.*, **42**, 813 (1992).
7. S. G. Hatzikiriakos, I. B. Kazatchkov, and D. Vlassopoulos, *J. Rheol.*, **41**, 1299 (1997).
8. P. A. Drda and S. Q. Wang, *Phys. Rev. Lett.*, **75**, 2698 (1995).
9. P. G. de Gennes, *C. R. Acad. Sci. Paris Serie B*, **288**, 219 (1979).
10. S. Q. Wang and P. A. Drda, *Macromolecules*, **29**, 2627 (1996).
11. F. Brochard-Wyart and P.G. de Gennes, *Langmuir*, **8**, 3033 (1992).
12. K. B. Migler, H. Hervet, and L. Leger, *Phys. Rev. Lett.*, **70**, 287 (1993).
13. S. G. Hatzikiriakos, *Intern. Polym. Proc.*, **IIX**, 135 (1993).
14. S. G. Hatzikiriakos and N. Kalogerakis, *Rheol. Acta*, **33**, 28 (1994).
15. J. R. A. Pearson, *Mechanics of Polymer Processing*, Elsevier, London (1985).
16. G. Georgiou and M. J. Crochet, *J. Rheology*, **38**, 639 (1994).
17. G. Georgiou and M. J. Crochet, *J. Rheology*, **38**, 1745 (1994).
18. K. A. Kumar and M. D. Graham, "The effect of pressure-dependent slip on flow curve multiplicity," *Rheol. Acta*, **37**, 245–255 (1998).
19. J. D. Shore, D. Ronis, L. Piché, and M. Grant, *Phys. Rev. Letters*, **77(4)**, 655 (1996).
20. J. D. Shore, D. Ronis, L. Piché, and M. Grant, *Phys. Rev. E*, **55(3)**, 2976 (1997).
21. W. B. Black and M. D. Graham, *Phys. Rev. Letters*, **77(5)**, 956 (1996).
22. G. C. Georgiou, *Rheol. Acta*, **35**, 39 (1996).
23. M. Fyrillas and G. Georgiou, *Rheol. Acta*, **37**, 61 (1998).
24. E. Brasseur, M. M. Fyrillas, G. C. Georgiou, and M. J. Crochet, *J. Rheology*, **42**, 549 (1998).
25. M. E. Cates, T. C. B. McLeish, and G. Marrucci, *Europhys. Lett.*, **36**, 845 (1992).
26. I. F. Berret, R. Gomez-Gorrales, J. Oberdisse, L. M. Walker, and P. Lindner, *Europhys. Lett.*, **41**, 677 (1998).